19951253 81

N95-31802

# CONTAMINATION DETECTION NDE FOR CLEANING PROCESS INSPECTION

W. J. Marinelli, V. DiCristina, D. Sonnenfroh and D. Blair
Physical Sciences Inc.
20 New England Business Center
Andover, MA 01810

## ABSTRACT

In the joining of multilayer materials, and in welding, the cleanliness of the joining surface may play a large role in the quality of the resulting bond. No non-intrusive techniques are currently available for the rapid measurement of contamination on large or irregularly shaped structures prior to the joining process. An innovative technique for the measurement of contaminant levels in these structures using laser based imaging is presented. The approach uses an ultraviolet excimer laser to illuminate large and/or irregular surface areas. The UV light induces fluorescence and is scattered from the contaminants. The illuminated area is viewed by an image-intensified CCD camera interfaced to a PC-based computer. The camera measures the fluorescence and/or scattering from the contaminants for comparison with established standards. Single shot measurements of contamination levels are possible. Hence, the technique may be used for on-line NDE testing during manufacturing processes.

## INTRODUCTION

The use of light-weight composite materials in structures which must function under extremes of temperature, pressure, and chemical environment presents new challenges to design engineers. Often these structures are of multilayered construction, with each layer conferring on the assembly specific properties. These types of materials range from common metals such as aluminum, matrix composites (MMC's) based on TiAl, beryllium, or copper, to ceramic reinforced carbon and silica based composites. In the joining of these multilayer materials and the welding of metals the cleanliness and structure of the interface can play a large role in the strength of the resulting bond. Contaminants may be present on these materials as a result of the manufacturing process or due to subsequent handling. Often, the simple process of oxidation during storage may substantially modify the surface structure. These contaminants may weaken adhesive bonding between layers via formation of a poor bond or via diffusion into one of the components. In the latter case the strength of the material may be compromised.

It is clear that non-destructive evaluation (NDE) techniques which can enhance the quality of bonded and welded structures in the assembly stage would greatly improve their strength and reliability. Furthermore, improved NDE techniques which enhance workplace productivity through reductions in rejected components or recognition of defective parts early in the assembly stage could substantially reduce manufacturing costs.

In this paper we discuss the development of a method which permits quantitative detection of contamination on bonding surfaces and which is capable of processing large, irregularly shaped surfaces, rapidly and in a non-destructive manner. The method is based on the principle that many of the contaminants will fluoresce when excited with UV light. However, unlike the traditional "black light" version of this principle used to detect contaminants, this method employs modern excitation and detection methods which can be readily quantified. The technique uses UV laser illumination of large surface areas to excite fluorescence in the contaminants. The use of the laser allows for much higher illumination intensities than previously employed using ordinary "black" light sources. The fluorescence excited by the laser is observed using a gated image-intensified television camera to provide a precise image of the object undergoing inspection. Thus, in a sense, a flash picture of the contaminants on the surface is recorded using this system without having to translate the item under inspection and without regard for the shape of the item. This image is collected in exposures on the order of 1s and captured

using a simple, PC-based, commercially available frame grabber system. The image may be used by process controllers to flag items for contaminant removal and the image can be filed and stored for NDE documentation purposes.

In the experiments described below we discuss the techniques used to select, quantitatively deposit, and image contaminants on a variety of manufacturing surfaces.

## EXPERIMENTAL

The experimental effort followed a series of sequential steps to optimize the effectiveness and determine the sensitivity of the technique for a representative set of contaminants and substrates. Optimization of the optical technique was accomplished by determining both the absorption and fluorescence spectra of the contaminants. From these spectra, excitation and detection wavelengths were selected for examination using fluorescence imaging. Fluorescence imaging experiments were performed by recording the fluorescence signal as a function of contaminant dosing level and illumination intensity. The technique was evaluated with respect to absolute sensitivity, contrast, and linearity of response. Additional measurements were performed in which larger structures were contaminated and viewed by the imaging system.

### Selection and Dosing of Contaminants and Surfaces

A specific goal of these measurements was the detection of Conoco HD-2 Calcium grease on D6AC steel, which is relevant to the bonding of the propellant liner to the Space Shuttle solid rocket motor (SRM). The full matrix of materials evaluated in the experiments is provided in Table 1 below.

Table 1. Contaminants and Substrates Examined Using Fluorescence Imaging

| | Substrate | | | |
|---|---|---|---|---|
| Contaminant | 6061 Al | D6AC Steel | NBR* | Quartz |
| Conoco HD-2 | X | X | X | X |
| Mineral oil | X | | | |
| DC 93-500 adhesive | X | X | X | X |
| Halocarbon wax | X | | | |

*Neoprene-butadiene rubber

Samples of the HD-2 grease were provided by Conoco. The mineral oil was spectroscopic grade and was purchased from Fisher Scientific. The DC93-500 adhesive is a special space-qualified, low outgassing RTV compound manufactured by Dow-Corning and specified by NASA and DOD for spacecraft use to reduce contamination effects. The halocarbon wax was purchased commercially from Halocarbon Products Inc. The composition of the wax was not specified by the vendor.

Precise contaminant dosing of the substrates was accomplished using modified techniques developed at the NASA Marshall Space Flight Center. Contaminants were diluted in a volatile solvent and applied to 2 x 2 $in.^2$ coupons of the substrate material using a Paasche #5 airbrush. The coupons were placed between a quartz crystal thin film monitor (QTFM) (Sycon Instruments Model STM-100) and two aluminum foil witness plates for determination of the dosing level. The contaminants were applied to the surfaces manually. Experiments were conducted to determine the spatial uniformity of the application technique and the fidelity of the QTFM in determining the dosing level. Less than 10%

non-uniformity was observed in the dosing of a 6 x 6 $in^2$ surface which enclosed the substrate coupon, QTFM, and aluminum foil witness plates.

The fidelity of the QTFM was verified by simultaneously dosing the QTFM and the two Al foil witness plates. The plates were weighted and compared with the mass gain inferred from the change in crystal oscillation frequency. These experiments could be performed without complication up to dosing levels of approximately 50 $\mu g/cm^2$. At this level the QTFM behaved erratically, indicating that there was poor coupling between the thick contaminant film and the crystal. Calibrations at higher dosing levels were performed by removing and cleaning the crystal prior to reaching the 50 $\mu g/cm^2$ limit. Additional dosings were then performed with the clean crystal. The dosing level was obtained from the sum of the readings prior to each cleaning cycle. The correlation between the mass gain inferred from the QTFM and the Al foil witness plates is better than 95%.

Absorption and Emission of Spectra of Contaminants

Contaminant absorption spectra were recorded using a standard laboratory spectrophotometer (Shimadzu UV-3100). The contaminants were applied to S1-UV quartz substrates (160 to 2200 nm transmission) using the spray station at dosings ranging from 100 to 150 $\mu g/cm^2$. The absorption spectra are presented over the relevant wavelength regions in Figure 1. The contaminants are observed to have absorption features primarily in the wavelength regions below approximately 250 nm, which is consistent with our expectation for aliphatic species. The spectra were analyzed using a Beer-Lambert Law type expression:

$$\ln(I_0/I_t) = \alpha\ T \qquad (1)$$

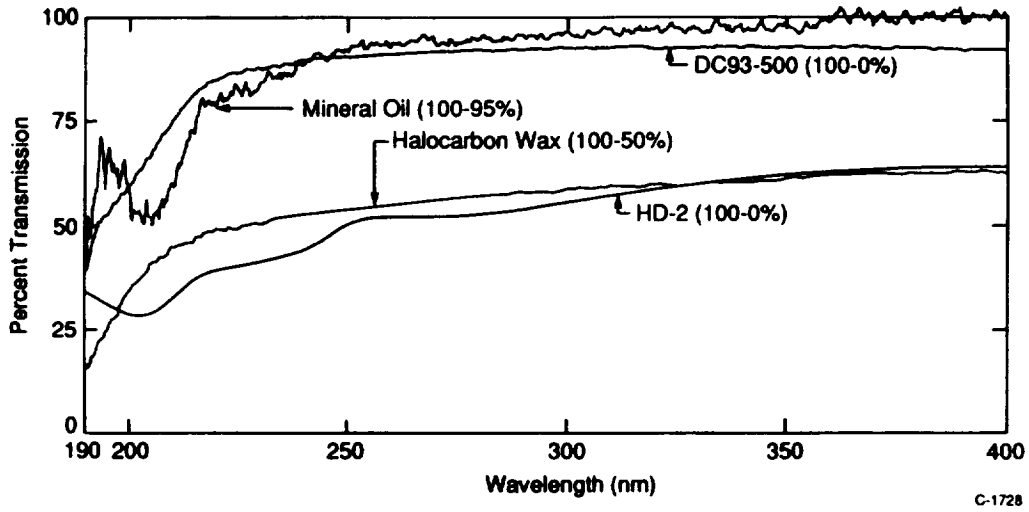


Fig. 1. Absorption spectra of HD-2 Grease, DC93-500, mineral oil, and halocarbon wax.

where $\alpha$ is the extinction coefficient in $cm^2/\mu g$, T is the film thickness in $\mu g/cm^2$ and $I_0$ and $I_t$ are the incident and transmitted light intensities. The extinction coefficient is comprised of two components, absorption of the light by the contaminant and scattering and reflection of the light by the layer. To first order, only absorption leads to fluorescence, although multiple scattering and further absorption within the medium will enhance absorption. Thus, the measured extinction coefficient represents an upper bound on the absorption by the film.

The optimum wavelength for the excitation and detection of these contaminants falls in the 190 to 240 nm region. Two high energy excitation sources produce light in this wavelength region: an

excimer laser operating on the ArF line at 193 nm and a UV flashlamp, which has emission throughout the UV and visible region of the spectrum. The ArF laser was used as source for excitation of the contaminants due to the close overlap between their absorption and emission bands.

The absorption spectra and the extinction coefficients indicate that a small fraction of the incident light is absorbed by the film, even for thicknesses as great at 150 $\mu g/cm^2$. Hence, the films are "optically thin" and attenuation of the excitation source through the layer is not an issue in the detection of the contaminants. The light absorbed by the film is simply:

$$I_a = I_0 - I_t \tag{2}$$

and by combining Expressions 1 and 2 we obtain

$$I_a = I_0[1 - \exp(-\alpha T)] \ . \tag{3}$$

In the optically thin limit ($\alpha T << 1$) Expression 3 reduces to

$$I_a = I_o \ \alpha \ T \ . \tag{4}$$

Hence, the absorbed intensity is linearly related to both the incident intensity and the contaminant film thickness in this regime. This is a primary feature of the fluorescence imaging technique.

Emission spectra were recorded by irradiating an S1-UV quartz plate coated with the contaminants at an angle of 45 degrees with respect to the surface normal using the 193 nm output from the excimer laser. Fluorescence from the coated substrate was viewed at 45 degrees from surface normal and 90 degrees with respect to the laser axis with a 0.3 meter scanning monochromator equipped with a photomultiplier tube (PMT). The fluorescence was collected with an f/4 UV lens and passed through a KBr disk to block scattered light from the laser while passing the fluorescence at wavelengths longer than 200 nm.

Emission spectra were recorded from 200 to 650 nm in two segments. A color filter was used to isolate the spectral orders of the monochromator. Spectra were recorded with coated and uncoated substrates and subtracted to eliminate substrate fluorescence effects, which were minor over most of the spectral region. The relative response of the spectrometer was calibrated using NBS- traceable deuterium and quartz-halogen emission standards. The emission spectra of the films are presented in Figure 2. The emission features are broad and all start from the short wavelength cutoff of the spectrometer and extend to approximately 400 nm. The relative intensities are qualitative, but show that the HD-2 and mineral oil samples are the strongest, followed by the DC93-500 and the halocarbon wax. The emission spectra of the contaminants indicated that a broadband UV filter which blocks the 193 nm laser light is optimum for detection of the contaminants. A Corning 7-54 color glass filter was chosen based on these considerations for use in these measurements.

The wavelength resolved emission spectra revealed that the primary regions of emission occur where the films do not strongly absorb radiation. Hence, there will be no "trapping" of the fluorescence by the film. The combination of "optical thinness" for both the excitation and emission wavelengths leads to a contaminant detection system which should have a linear response over a broad range of contaminant levels. To first order, the observed fluorescence intensity can be related to the absorbed intensity via the expression

$$S_F = I_0 \ \alpha \ T \ \Phi_f \ A_o \ \Omega_o \ \tau_o \ Q_e \ / N_p \tag{5}$$

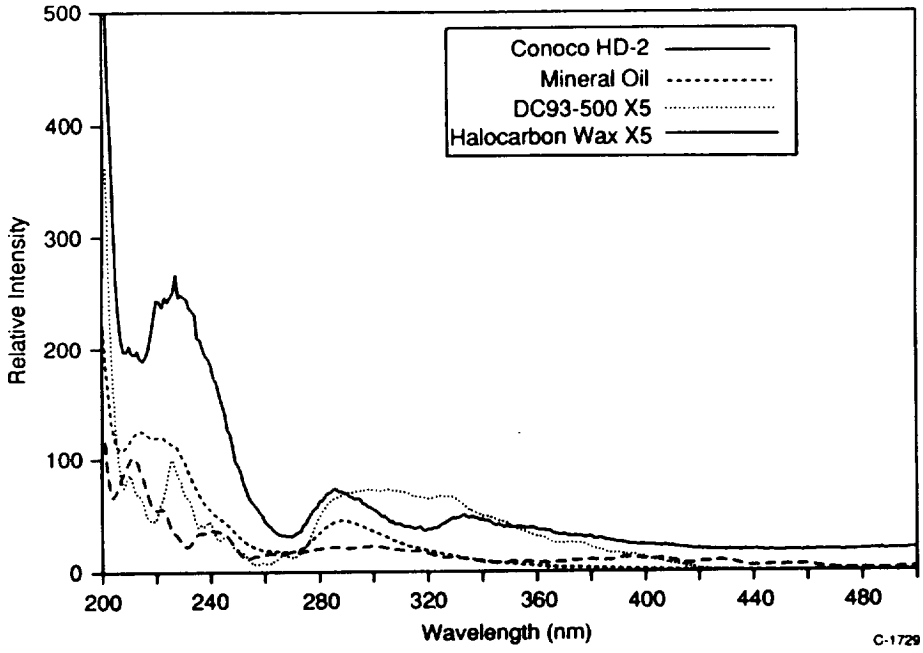


Fig. 2. Emission spectra of HD-2, mineral oil, DC93-500, and halocarbon wax excited at 193 nm.

where

$\Phi_f$ is the fluorescence efficiency for the contaminant,
$A_o$ is the aperture of the fluorescence collection optics,
$\Omega_o$ is the steradiancy (field of view) of the detection system,
$\tau_o$ is the transmission of the optics and filters,
$Q_e$ is the quantum efficiency of the detection system,
$N_p$ is the number of pixels in the detector for imaging,

and where these quantities have been averaged across the bandwidth of the detection system, as appropriate. The reduction in $S_F$ by $N_p$ assumes that the detection system is viewing a spatially homogenous field. Of course, this is not a requirement of the system but it does place a lower bound on the signal levels.

The fluorescence efficiency, $\Phi_f$, is given by the ratio of the fluorescence emission rate to the total rate of decay of the fluorescing state. The primary influence on the fluorescence efficiency is the rate at which the excited state is quenched by the surrounding molecules. Except for those molecules which are quite close to the surface of the substrate or the air interface, the environment around the excited state is constant, and hence so is $\Phi_f$. Only for extremely thin layers should the efficiency deviate from a constant value. The thickness at which this effect becomes important can not be predicted, a priori, but would be observed in the measurements as a curvature in the response of the system at low contaminant levels.

Optical Detection of Contaminants

Experiments were conducted to determine the energy and concentration dependence of the fluorescence signal from the contaminants on the substrates previously described. The experimental apparatus is shown schematically in Figure 3. The apparatus can be described in terms of an excitation system, a fluorescence detection system, and a diagnostics system.

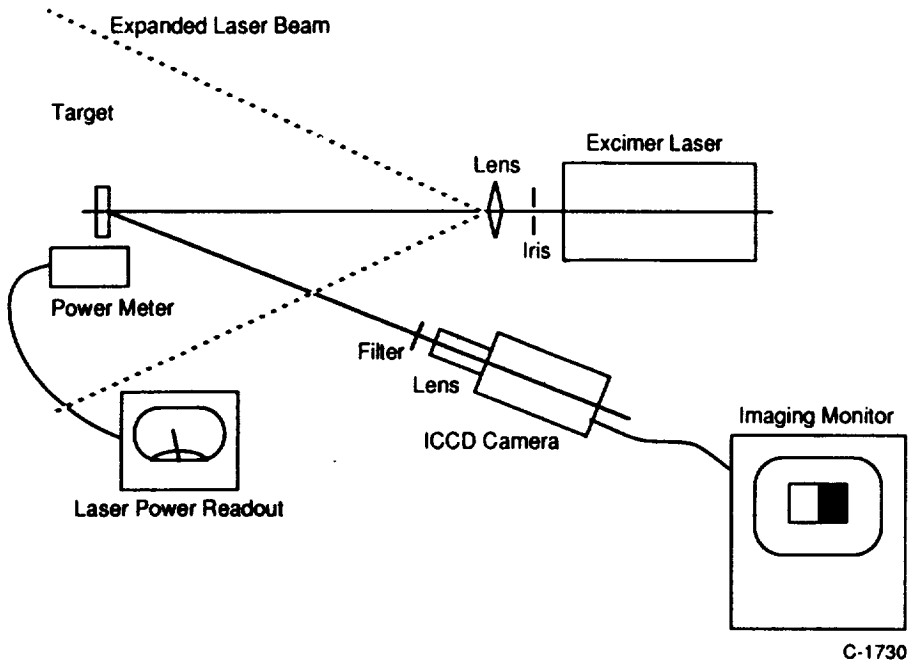


Fig. 3. Experimental fluorescence imaging apparatus using an ArF excimer laser and gated, image-intensified CCD camera.

The excitation system consisted of a rare gas halide excimer laser (Questek Model 2820) operated on the ArF line at 193 nm. The laser output energy was 200 mJ/pulse at a repetition rate of 10 pulses per second. The pulse duration was approximately 20 ns. The laser beam was rectangular (5 x 20 mm) and moderately divergent. A lens was placed at the beam exit port of the laser, causing the beam to come to a focus and then diverge as it illuminated the target substrate, which was located approximately 150 cm from the lens.

The substrate was typically a 2 x 2 $in.^2$ coupon mounted on an optical post in the beam path. The laser beam fully illuminated the target substrate. A surface absorbing power meter (Scientech 36-0001) could be substituted in place of the target to measure the laser energy incident at the illumination plane. For these measurements the laser fluence was typically 100 $\mu J/cm^2$/pulse. The 2 x 2 $in.^2$ coupons were dosed using the system described previously. A mask was applied to one half of the coupon during application of the contaminant in order to provide a clean surface reference for each measurement. The sample coupon was dosed sequentially, with increasing amounts of the contaminants, when constructing a calibration curve. Repeated exposure to the UV light had no observable effect on the behavior of the films, with the exception of the DC93-500 silicone dosed substrates, which will be discussed later.

Contaminant fluorescence was observed using an intensified and cooled CCD camera (Princeton Instruments). The pixel resolution of the camera was 526 x 384. The intensifier was gated to match the duration of the fluorescence signal, which was typically 1 to 2 μs. Gating of the detection system was also a key factor in excluding background illumination from the image. A 105 mm f/4.5 UV imaging lens (Nikon) interfaced to the camera, was used to capture the fluorescence from the films. The Corning 7-54 color filter was mounted at the entrance to the lens. In some experiments, a 35-105 mm standard zoom lens (Nikon) was used to widen the field of view of the detection system in order to observe

contamination levels on larger objects. This capability was achieved at the expense of approximately a factor of 7 in sensitivity due to the reduced UV transmission of the glass optics in the lens.

The camera was interfaced to a computerized data acquisition system consisting of a PC type computer (Gateway 2000 486/33) operating on software furnished with the camera by Princeton Instruments. The software allowed for the acquisition of fluorescence images from single pulses of the laser. For weaker signals multiple pulses could be averaged on the camera chip or in computer memory. In most cases, single shot fluorescence intensities provided sufficient signal levels to meet the detection goals. Fluorescence intensities for the dosed and clean sides of the coupon were processed by the camera system to obtain signal levels (counts) per pixel. A simple subtraction of the two signals yielded the fluorescence intensity due to the contaminant alone as a function of position on the coupon. A false color scale could be applied to the image to indicate the absolute level of contamination, given the proper calibration factors. Images could be stored in memory for further processing, photographed for presentation, or used to produce contour plots of the contamination levels.

The detection of HD-2 grease was the primary focus of the effort. Figure 4 shows the fluorescence intensity per pixel as a function of contaminant level for HD-2 on the aluminum, D6AC steel, quartz, and NBR substrates. Signal levels range from a high of 10,000 counts/pixel, where the camera saturates, to less than 100 counts/pixel over a concentration range from 0.1 to 100 $\mu g/cm^2$. A least-squares fit to the data on these log-log plots indicate that the signal is linearly proportional to the contaminant level, within experimental accuracy, over nearly three orders of magnitude. Furthermore, the linearity is independent of the identity of the substrate, i.e., the technique is equally applicable to insulating materials. The contrast between the dosed and clean sides of the substrate is excellent, and greater than 5 even at the lowest dosing levels considered.

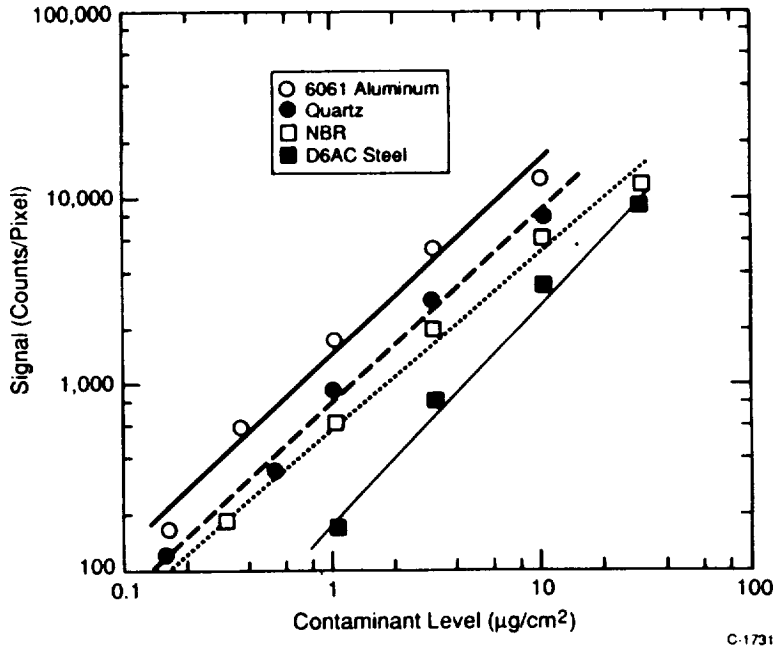


Fig. 4. Fluorescence signal as a function of HD-2 contaminant level for various substrates.

The behavior of the fluorescence as a function of laser illumination level is provided in Figure 5 for the Al substrate. The intensity is observed to be a linear function of the laser intensity for aluminum as well as all of the substrates considered.

A lesser set of data was recorded for the detection of mineral oil, since it appeared to behave similarly to HD-2. As with the HD-2, the response of the fluorescence detection system is linear, within experimental error, as a function of both contaminant level and laser intensity.

Unanticipated problems arose in the detection of DC93-500 silicone adhesive. The fluorescence signal was strong but behaved erratically. Further investigation revealed that photochemical processing of the adhesive by the UV light was altering the composition of the film. This effect is most likely due to photochemical polymerization of the unreacted monomers in the contaminant layer. The effect was most pronounced for the D6AC steel, where a chemical interaction with the substrate produced a black layer which did not fluoresce. We believe this anomalous behavior is an artifact of the contaminant preparation method rather than an indication of the true response of the system to the silicone impurities. Our preparation technique allowed a high level of unpolymerized compound to be deposited on the surface. Normal polymerization of the RTV adhesive is via a radical catalyst. The photochemical production of these radicals by the laser promotes the further catalysis of the polymer, which was arrested by the dilution of the reacting mixture in the solvent at the time the sample was prepared.

Detection of fluorocarbon wax by this technique proved quite difficult. Both the absorption and emission spectra indicated a weak response to light at 193 nm. The indications were confirmed when little or no signal was observed with the fluorocarbon wax. Our previous experience in imaging a fluorocarbon based vacuum grease had shown some promise. Hence, further examination of these compounds is warranted before excluding their detection by this technique.

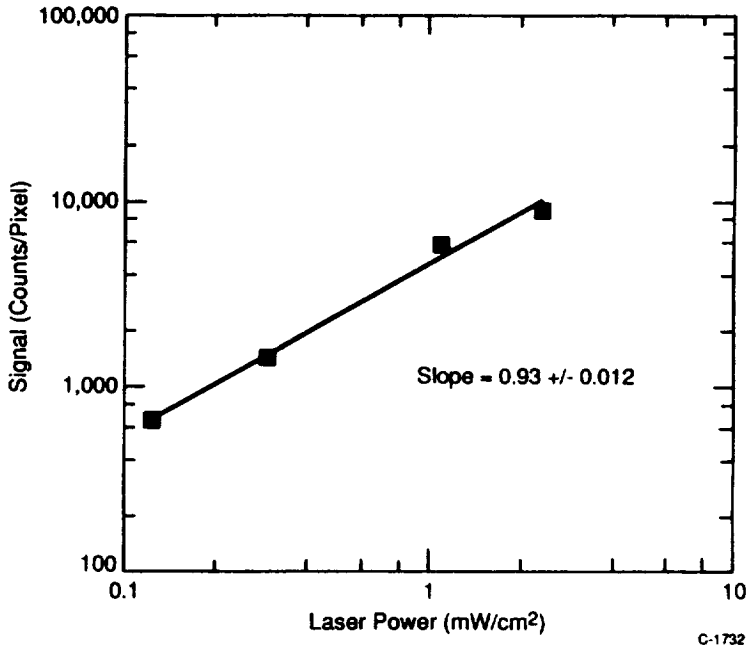


Fig. 5. Dependence of the fluorescence signal on laser intensity for a 6061 aluminum substrate.

## DISCUSSION

The fluorescence imaging results presented in this report verify the physical model of contaminant fluorescence based on simple absorption and emission of radiation in the optically thin limit. The model predicts a linear dependence of the contaminant fluorescence signal on contaminant level and illumination intensity. Our assumption that the technique was equally applicable on insulating and conducting surfaces was also verified. The influence of surface structure on the fluorescence signal

was clearly evident in the data. As demonstrated in Figure 4, HD-2 grease fluorescence on 6061 aluminum is much stronger than on D6AC steel for comparable dosing and illumination intensities.

Two rather simple explanations might be offered to account for the differences. The first explanation considers the surface reflectance of aluminum compared to D6AC steel. The aluminum appears visually to be highly reflective. In contrast, the D6AC steel is black and has a grit blasted surface which acts as a good light trap. A highly reflective surface can effectively double the apparent light path through the contaminant. In the optically thin limit of contaminant absorption, this effect would increase the fluorescence signal on the aluminum by a factor of two compared to the steel for normal incidence by the light source. While this explanation is plausible, it is not consistent with the fluorescence data recorded on the quartz (smooth and transmissive) and NBR (smooth and absorbing) substrates. The absolute sensitivity for HD-2 grease on both these smooth surfaces is virtually identical to the absolute sensitivity measured for HD-2 on the aluminum substrate. Hence, we must conclude that the aluminum is not highly reflective at 193 nm and that the fluorescence signal is due completely to the first transit of the contaminant film by the excitation light.

The second explanation for the apparent decreased sensitivity on D6AC steel is due to the increased surface roughness of the sample. Since the surface is highly roughened (approx. 100 μin. scale size), the effective surface area is much higher for a 2 x 2 $in.^2$ coupon of the steel compared to the Al. The contaminant dosing assumes a smooth surface, hence the effective dosing level per unit surface area is reduced due to the surface roughness. Similarly, the intensity of the light incident on the surface is reduced by this same roughness factor. However, the projection of a camera pixel onto the roughened surface will incorporate the total mass and the total energy deposited into the area. Hence, the effects of surface roughness should cancel in the optical detection system.

A second influence of the surface roughness may be in the coupling of the electronic energy in the contaminant molecules to the underlying substrate. For the roughened surface the effective thickness of the contaminant layer is reduced and the contaminant may interact with the surface to a much greater extent. The coupling of the molecular electronic energy to the surface acts to reduce the fluorescence quantum efficiency. The reduced fluorescence efficiency translates into a reduced detection sensitivity for the film. One impact of this phenomenon would be a non-linear dependence of the fluorescence signal on film thickness, since the range to the underlying substrate increases and its influence should decrease. The correlation of the fluorescence signal with the film dosing level for HD-2 on D6AC steel is somewhat greater than linear. However, the uncertainty in the correlation is with the limits of a linear response. Further data would be required to definitively establish the correlation. Data on the dependence of the signals on surface roughness and fluorescence excitation and viewing angles are also desirable to understand the response on D6AC steel. The acquisition of this data was beyond the scope of the current effort.

The focus of our initial efforts was in the detection of specific isolated contaminants on a range of substrates. A key issue in the implementation of the diagnostic will be the ability to detect multiple contaminants, perhaps with different detection efficiencies. The data indicate that differentiation of contaminants will be extremely difficult in most cases. The absorption and emission bands for the contaminants examined in this effort had few features which might enable differentiation between compound types. Specific identification of compounds would not be possible except in well defined scenarios. We also did not examine any synergism between mixed contaminants on a surface. This synergism can influence the fluorescence signal as an enhancing factor, in which energy is transferred from an absorbing molecule to one which fluoresces with greater efficiency. A similar energy transfer mechanism could reduce the signal if energy was transferred to a compound which did not fluoresce or emitted light in a spectral region outside the detection system bandpass. In general, the diagnostic is best suited for situations in which the range of contaminants which might be present on the bonding surface is reasonably well defined. This condition is present in a large number of bonding and manufacturing tasks.

## CONCLUSIONS

The use of UV fluorescence imaging of contaminants on bonding surfaces has a high degree of sensitivity, a linear response with contaminant level and light intensity, and is independent of substrate material. Large and irregularly shaped objects can be imaged with the technique, often without any rastering of the detection system or object required. Calibrated false color-encoded images of the surfaces can be provided with existing software. The system has been demonstrated to detect Conoco HD-2 grease on grit-blasted D6AC steel, 6061 aluminum, and NBR with sensitivity as low as 0.1 $\mu g/cm^2$ (0.11 $mg/ft^2$) with a spatial resolution of 1 $mm^2$. This capability has direct application to quality control in the maintenance of Shuttle solid rocket motors.

## ACKNOWLEDGEMENTS

This work was funded by the NASA Langley Research Center, and NASA Marshall Spaceflight Center under the Small Business Innovative Research Program. The author wishes to thank Thomas Yost at NASA langley, Chris Welch at William and Mary, and Billy Nerren at NASA Marshall for their assistance and support of this effort.

# CLEANING VERIFICATION—INSTRUMENTATION AND TECHNIQUES 2